METEOCAST: A NEURAL ENSEMBLE NOWCASTING MODEL BASED ON GEOSTATIONARY MULTISPECTRAL IMAGERY FOR HYDRO-METEOROLOGICAL APPLICATIONS

Michele de Rosa[1,2],Frank Silvio Marzano[1]

(1) "Sapienza" University of Rome, via Eudossiana, 18 - 00184 Rome – Italy
(2) GEO-K srl, via del Politecnico, 1 – 00133 Rome – Italy

Abstract

The modern Numerical Weather Prediction (NWP) models used to predict the weather conditions work on large scales both in time and space. On the other hand, meteorological events, like the thunderstorms, develop on small scales because they last from a few minutes to a few hours and they develop from a few hundred meters to some kilometres. For these reasons, it is clear that the NWP models are insufficient in order to achieve a good prediction of the extreme meteorological events and it is necessary to use other kind of models, which are able to give high resolution (in space and in time) predictions with a given degree of confidence. The objective of this work is to propose, develop and validate a new predictive model, based upon satellite observation. The Meteosat Second Generation (MSG) satellite is the data source. Its high resolution both in time and space gives the possibility to satisfy some of the requirements needed to nowcast the development of extreme meteorological events and, in a more wide view, gives the possibility to monitor the environment in an efficient way and to plan actions in the case of dangerous events. This work discusses a new kind of model, named MeteoCAST (Meteorological Combined Algorithm for Storm Tracking) and it shows some possible applications:

- the 1-hour ahead nowcasting of the cloud coverage
- the 1-hour ahead nowcasting of the rain rate

The prediction model is based on an Ensemble framework, the Dynamically Averaging Networks (DAN) ensemble, which uses a set of simpler cooperating models. These models use the Infrared MSG channels to make the satellite image prediction, while the cloud coverage classifier and the rain field estimator, based on the neural networks framework, use the ensemble output in a waterfall manner. The estimators are integrated with the Satellite Application Facility (NWCSAF) framework.

INTRODUCTION

NOWCASTING of rainfall from remote sensing imagery is becoming an important issue for several applications, which are mainly related to civil protection alarming and also to hydro-meteorological applications [1]-[4]. The term nowcasting should be intended, in this context, as the ability to predict, at very short-term time scales, the evolution of the geophysical field of interest from remote sensing imagery. For a rapidly varying field, such as rainfall, high temporal repetition of the observation, like that available from geostationary satellites, is essential [8]. On the other hand, the accuracy of the nowcasted fields is strictly related to the physical correlation of the measured remotely sensed data with the field of interest [9]-[11]. The rainfall nowcasting problem from the satellite remote passive sensors can be conveniently split into two basic components as follows: 1) instantaneous retrieval; and 2) temporal prediction. Several rain retrieval techniques have been proposed on the basis of multi-satellite imagery, exploiting passive sensor measurements acquired by geostationary Earth orbit (GEO) and low Earth orbit (LEO) platforms [8]-[14]. These approaches tend to overcome some inherent limitations due to the use of satellite infrared (IR) radiances, which are poorly correlated with

rainfall [6]. In this respect, microwave (MW) radiometric data available from LEO platforms can provide more accurate rain estimates [15]. From a microphysical point of view, visible (VIS) and IR radiometers can give information on cloud top layers since precipitating clouds are almost completely opaque are in the IR. On the other hand, MW radiometers can detect cloud structure and, to some extent, near-surface rainfall. From a system point of view, GEO satellites can ensure Earth coverage with a high temporal sampling, whereas LEO satellites have the advantage to enable the use of MW sensors but with the drawback of low temporal sampling. Therefore, LEO-MW and GEO-IR radiometries are clearly complementary in monitoring the Earth's atmosphere and a highly variable phenomenon such as precipitation. The IR radiances from geostationary images can be properly calibrated using the MW-based combined algorithms (e.g., [5] and [13]-[16]). Microwave data can be extracted from the MW imager sensors, but any rain estimation source may be used [9]. Rainfall nowcasting by active and passive remote sensing imagery has been attempted by numerous techniques in the last decade [3], [4], [17], [18]. On the other side the need to overcome the low sampling of the LEO satellites has brought to the development of rainfall estimation algorithms, like the NWCSAF Convective Rainfall Rate (CRR) [26], which are synchronous with the GEO satellites. Some of the proposed nowcast methods may be classified as standard, such as the temporal image persistence (TIP) and steady-state displacement (SSD) (e.g., [17]). Each of these conventional nowcasting methods shows a performance that depends on the weather conditions in the considered region.

The basic aim of this paper is to exploit the potential of the ensemble technique to both predict and retrieve the rainfall pattern using GEO satellite, the MSG satellite, and the CRR. Great attention has been placed to select the input space-time features and the optimization of the ensemble parameters in order to optimize the rainfall nowcasting performance from the satellite imagery temporal sequences with respect to the conventional approaches. The goal of the proposed technique is to describe a general ensemble technique that is flexible, general and quickly available.

METHOD

The approach followed to build the nowcasting framework, shown in Figure 1, is bottom-up.

First of all the ensemble model has been setup in order to be used for the MSG images nowcasting from 30 minutes to 60 minutes. After a cloud classifier has been trained in order to classify each pixel of a MSG image and finally a rain rate estimator has been setup in order to estimate the rain rate on the cloudy pixels using the NWCSAF Convective Rainfall Rate.

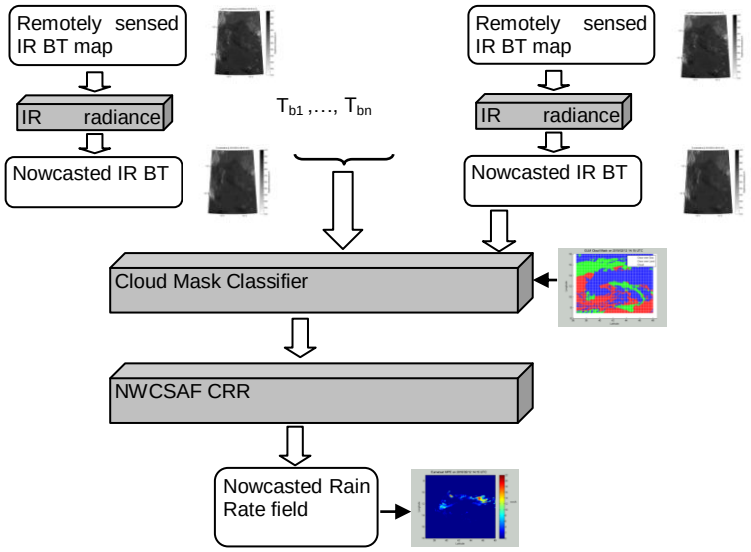

Figure 1: *The MeteoCAST logical layout: the flow goes from the MSG images acquisition to the rain rate estimation.*

NOWCASTING ARCHITECTURE

The chosen ensemble architecture is shown in Figure 2:

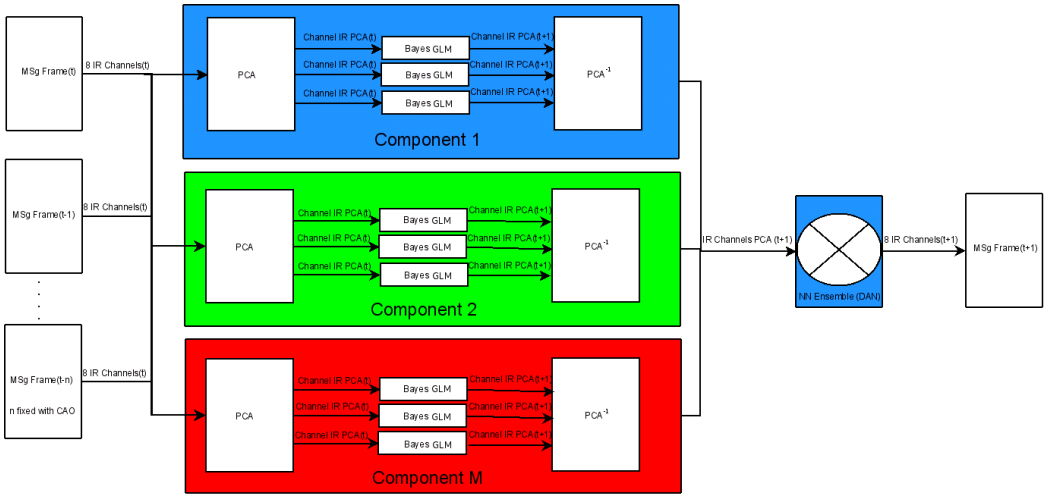

Figure 2: **The nowcasting architecture. The frames in input are broadcasted to each ensemble's components and the output of each component is mixed to give the ensemble's output.**

It is clear that the ensemble paradigm is fully embedded in Figure 2. The temporal window was found using the Cao method [21] to discover the optimal embedding dimension. This dimension is the number of images in the past related to the current frame. This number has been fixed to 6 images or 90 minutes in the past. According to it, the MSG frames are given in input to the ensemble. The MSG IR channels are compressed using the PCA [22] in order to speed-up the computation time and then dispatched to each ensemble's component. Each component is a Generalized Linear Model (GLM) [23], which is trained using the Bayesian Framework [24] and the NeuCAST's approach [25]. Each component gives its own prediction and each output is mixed following the Dynamically Average Network (DAN) approach [26].

GENERALIZED LINEAR MODELS

The base model used as ensemble's components is the Generalized Linear Model (GLM) [23], which can be written in the form:

$$E(Y) = \mu = g^{-1}(\eta) \qquad \textbf{(1)}$$

The GLM generalizes linear regression by allowing the linear model to be related to the response variable via a link function g , while the other components of the models are: 1) a distribution function *f*, from the exponential family and 2) a linear predictor $\eta = \mathbf{X}\boldsymbol{\beta}$.

In a GLM, each outcome of the dependent variables, Y , is assumed to be generated from a particular distribution function in the exponential family; a large range of probability distributions that includes the normal, binomial and Poisson distributions, among others.

The model chosen sets the identity function as link and *f* is the Gaussian distribution. So the GLM could be written in the form:

$$y(x;w) = \sum_{j=1}^{M} w_j \phi(x_j) = W^T \Phi(X) \qquad \textbf{(2)}$$

where $\phi(x)$ is a linear function.

The Bayesian framework [24], used to train the GLM model, implements the Occam razor in order to penalize the model overall complex versus simpler models. It applies two steps to find the best model mapping the data:

1. Fit the model to the data. This is the training step.
2. Compute the evidence to find the best model. This is the regularization step.

Finally in order to minimize the amount of information regarding the IR channels a Principal Components Analysis (PCA) [22] has been applied. This technique applies a linear transformation on the data and it has the advantage of reduce the number of channels, but it is a loss of information technique, because it penalizes the components of the data which aren't representative of the data.

THE ENSEMBLE NOWCASTING METHODS

The ensemble of models is a composition of different models (the ensemble's components) whose outputs are mixed to give the output of the ensemble. Given *L* components, the general form of the ensemble is the General Ensemble Model (GEM) [19][26] which has the following form:

$$f_{GEM} = \sum_{i=1}^{L} \alpha_i f_i(x) \qquad \textbf{(3)}$$

In general the mixed coefficients α_i are constrained by the following conditions:

1) $0 \le \alpha_i \le 1$

and

2) $\sum_{i=1}^{L} \alpha_i = 1.$

These two conditions guarantees that the output of (4) is a weighted sum of its components.
The naive form of the GEM is the Basic Ensemble Model (BEM) which has the following form:

$$f_{BEM} = \frac{1}{n} \sum_{i=1}^{L} f_i(x) \qquad \textbf{(4)}$$

It is possible to show that the average sum-of-square error introduced by the GEM and the average sum-of-square error introduced by the BEM have the relation:

$$\mathrm{E}_{GEM} \le \mathrm{E}_{BEM} \qquad \textbf{(5)}$$

The approach used in this work is named Dynamically Averaging Networks (DAN) [26] and it is a special case of the GEM. The form of the DAN is the following:

$$f_{DAN} = \sum_{i=1}^{L} w_i f_i(x) \qquad \textbf{(6)}$$

where

$$w_i = \frac{c(p_{f_i})}{\sum_{j=1}^{L} c(p_{f_j})} \qquad \textbf{(7)}$$

and $c(p_{f_i})$ is the certainty function defined as follows:

$$c(p_{f_i}) = \begin{cases} p_{f_i} & \text{if } p_{f_i} \ge 0.5 \\ 1 - p_{f_i} & \text{otherwise} \end{cases} \qquad \textbf{(8)}$$

In the DAN approach the parameters or weights are not fixed a priori, but are computed dynamically every time a new output appears.
To apply the DAN, it should be possible to assign a probability to each output of the ensemble's components, in order to compute the certainty function. If $Err_i(f_i)$ is the error bar related to the output of the component *i* then it should be possible to assign a probability to each output as follows:

$$p_i(f_i) = \frac{Err_i(f_i)}{\sum_{j=1}^{L} Err_j(f_j)} \qquad \textbf{(9)}$$

It is possible to show [19] that:

$$1 \le \mathrm{E}_{DAN} \le \mathrm{E}_{GEM} + 1 \qquad \textbf{(10)}$$

THE PERFORMANCE INDEXES AND THE BENCHMARKS

The performance indexes used to measure the quality of the predicted image are the following: the BIAS, the RMSE and the Correlation Index, while the benchmarks used to compare the image prediction are the Persistence [17] and the Steady State Displacement (SSD) [17]. The Persistence method considers the current frame as the nowcasted image while the SSD method tries to estimate the motion vector and applies it to the current image in order to compute the predicted image.

GEOSTATIONARY SATELLITE DATA

The data related to the brightness temperature are taken from the 8 IR channels of the MSG 8,9 and 10, while the data related to the rain field are taken from the run of the NWCSAF CRR product [26].
The Meteosat 8, 9 and 10 Spinning Enhanced Visible and InfraRed Imager (SEVIRI) has been considered As a source of GEO satellite imagery, selecting the area of interest centred in Southern Europe. The selected IR MSG image frames are composed of 275 × 344 pixels, corresponding roughly to east longitude ranging from 7° to 18° and north latitude ranging from 36.5° to 48°. Each SEVIRI pixel can be approximated by a square of 3 × 3 km at mid latitudes.
The Convective Rainfall Rate product is generated by the NWCSAF framework [26] which is able to estimate the instantaneous rainfall rate field from the MSG images.

THE CASE STUDIES

The case studies are related to some meteorological events within the Mediterranean Sea (Italy) and they are divided into two groups: the first group is used to train the model related to the MSG images (image nowcasting) and the second group considers very interesting meteorological events (like snow and thunderstorms).
The events belonging to the first group are the following:

1. July 24th, 2006: training case
2. August 13th, 2006: training case
3. September 14th, 2006: training case
4. May 3th, 2010: validation case

The first event is related to a strong thunderstorm activity over the Italy, while the other events are related to cloud motion over the Italy with heavy and moderate rain.
The fourth event is related to a tornado over the Modena city in the Northern of Italy. The event started to develop at 13:00 UTC and it ended at 16:00 UTC. Several damages occurred and some people were injured.

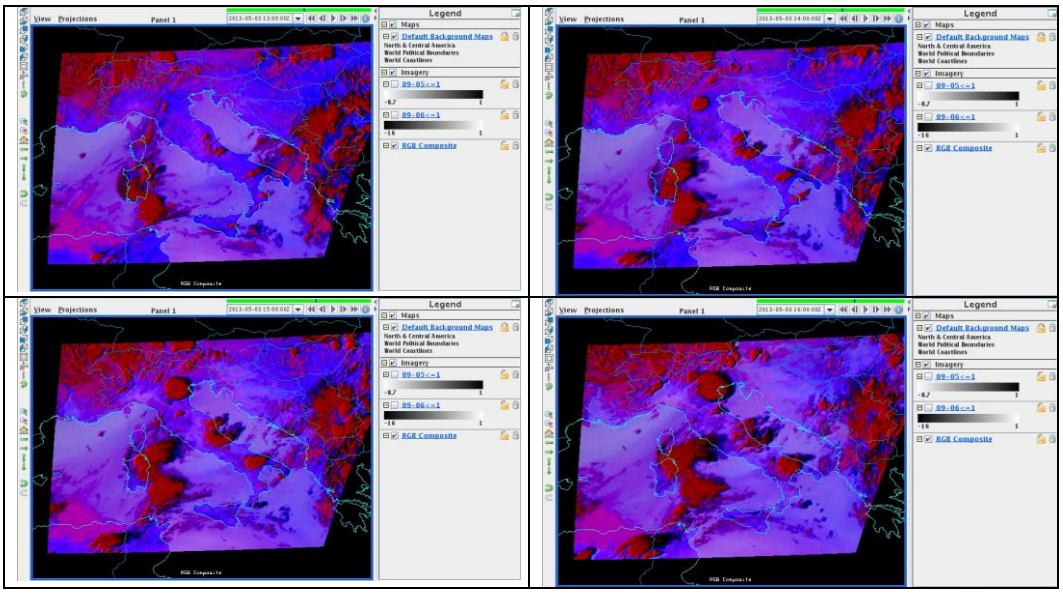

Table 1: **IR MSG RGB images related to the tornado event over Modena on 2013/05/03**

THE RESULTS FOR THE TRAINING SET

Using the Persistence and the SSD as benchmarks, the performance indexes have been computed over the training case studies in order to assess the goodness of training of the model.

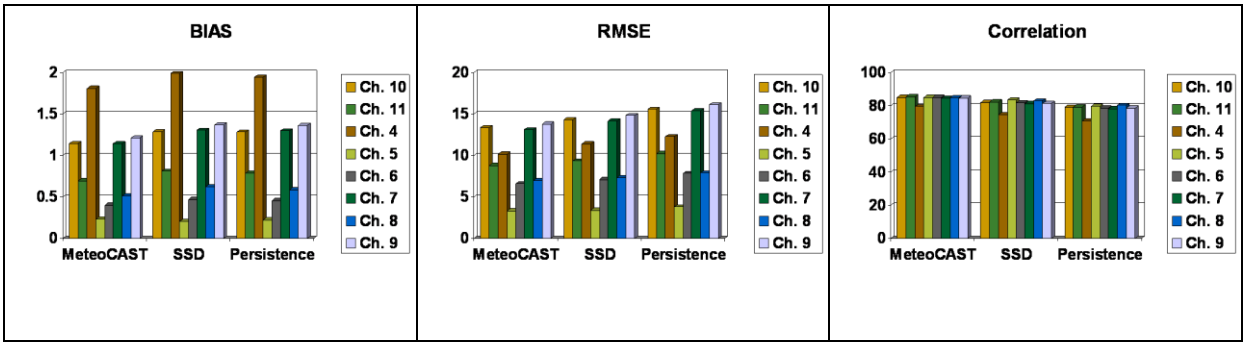

Table 2: **The performance indexes over the training set computed for each benchmark against the true MSG image.**

The Table 2 shows a very good performance of the MeteoCAST model compared to the benchmarks especially for the RMSE and the Correlation indexes, while the BIAS performance is comparable with the Persistence and the SSD.

THE RESULTS FOR THE TORNADO

The performance indexes for the tornado event are computed as in the previous section and the results are shown in the Table 3
:

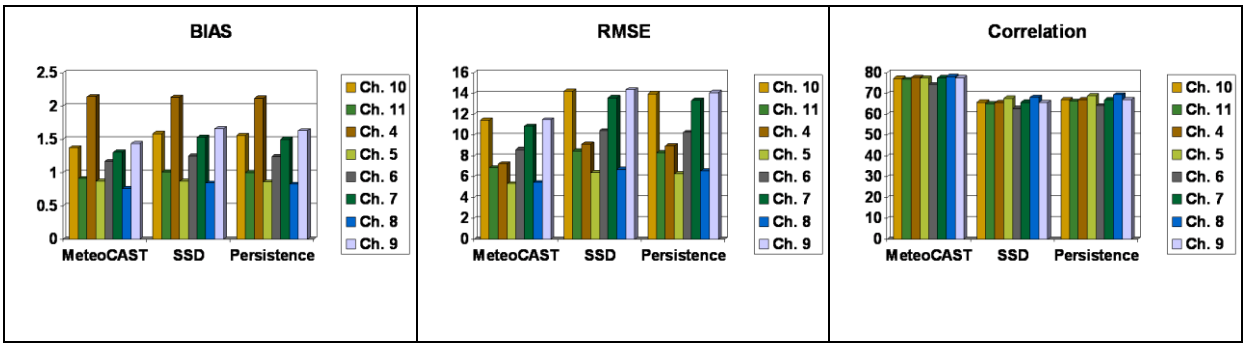

Table 3: **The performance indexes over the tornado event at 14:00 UTC computed for each benchmark against the true MSG image.**

The indexes are very good for the MeteoCAST compared to the benchmarks, overall for the correlation index which peaks at 80% (more than 10% above the Persistence and the SSD). The reasons of this difference are related to the loss of the correlation between the MSG images during the event that influences the two benchmarks. On the other hand this shows the high reliability of the MeteoCAST model in different situations. Finally the synthetic images, produced in the previous steps, are used in order to estimate the rain rate field in a waterfall manner using the three level of computation.

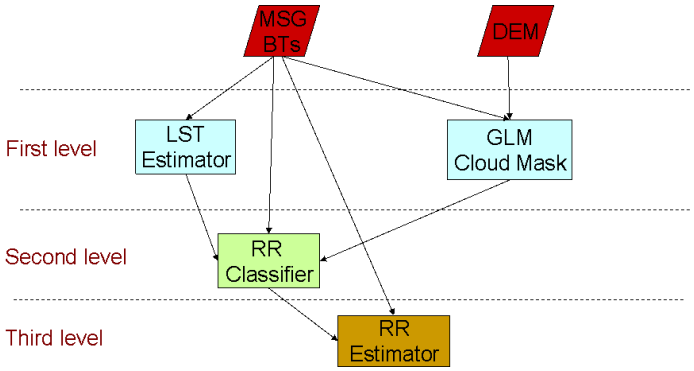

Figure 3: **The computational flow of the rainfall estimation**

The estimation is done using the Convective Rainfall Rate product of the NWCSAF in order to recalibrate the neural models.

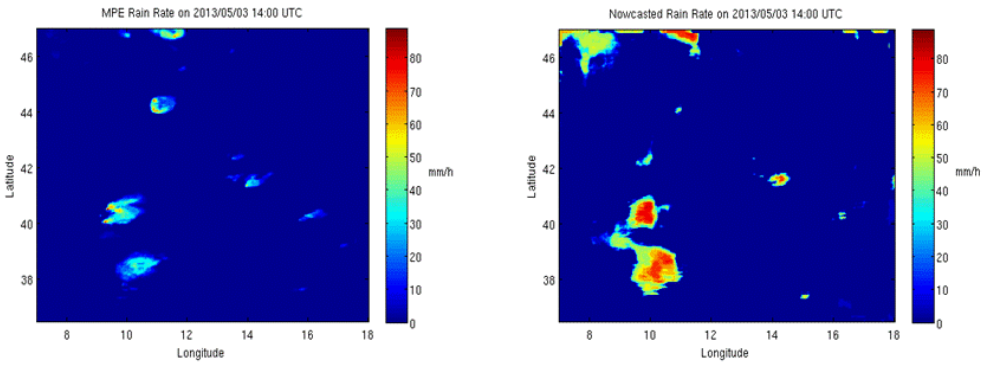

Performance Indexes 60 Min		
BIAS	2.17	mm/h
RMSE	10.49	mm/h
Correlation	53.00	%

Figure 4: **Rainfall estimation using the NWCSAF CRR product.**

The indexes are computed using the Multisensor Precipitation Estimate (MPE) Eumetsat product. The comparison shows a poor relation of the reconstructed field. These performances are probably due to the high spatial and temporal variation of the event which is well reflected into the channels reconstruction but poorly at product level. A case with a lower dynamics performs better as described by Figure 5:

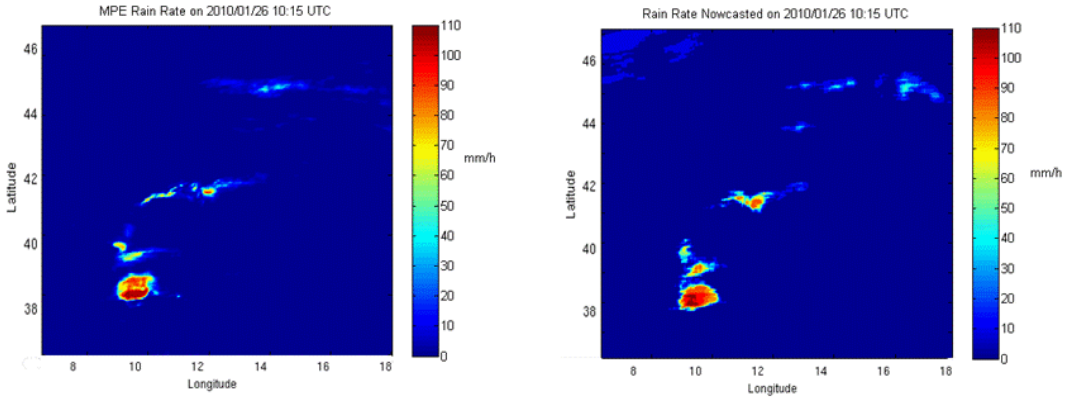

Performance Indexes 60 Min		
BIAS	1.33	mm/h
RMSE	9.05	mm/h
Correlation	68.47	%

Figure 5: **A more static rainfall case. On the right side the MPE product and on the right side the MeteoCAST rainfall field predicted.**

CONCLUSIONS

In this paper a new nowcasting model, named MeteoCAST, is presented and discussed. The model produces synthetic forecasted MSG images which could be used to nowcast the rainfall. The technique is applied on a very dynamic event like a tornado and the result at satellite image reconstruction level are very good, while they are poor at rainfall product level. This is due to the high

dynamics of the event as showed by the field reconstruction on a more static case. The plan for the future developments of the model is related to the full integration with the NWCSAF framework, the use of the Rapid Scan Service and the extension to the “90 minutes ahead” forecast.

ACKNOWLEDGEMENTS

Thanks to the Italian Air Force Meteorological Office for the support.

REFERENCES

[1] G. Roth, G. Boni, F. Giannoni and R. Rudari, “On the role of a hydrologic model in regional precipitation and flood frequency analyses, EOS”, *Trans.AGU*, vol. 85(17), JA259, 2004.
[2] F. Siccardi; G. Boni; L. Ferraris; and R. Rudari, “A hydrometeorological approach for probabilistic flood forecast”, *J. Geophys. Res*., Vol. 110, No. D5, D05101, 2004.
[3] L. Li, W. Schmid, and J. Joss, “Nowcasting of motion and growth of precipitation with radar over a complex orography,” *J. Appl. Meteorol*., vol. 34, pp. 1286–1300, June 1995.
[4] J. W. Wilson, N. A. Crook, C. K. Mueller, J. Sun, and M. Dixon, “Nowcasting thunderstorms: A status report”, *Bull. Amer. Meteor. Soc*., vol. 79, n. 10, pp. 2079-2099, 1998. F.S. Marzano, A. Mugnai and J. Turk, “Precipitation retrieval from spaceborne microwave radiometers and combined sensors”, in *Remote ensing of atmosphere and ocean from space*, F.S. Marzano and G. Visconti Eds., Kluwer Academic Publ., Dordrecht (NL), pp. 107-126, 2002.
[5] G.A. Vicente, R.A. Cofield, and W.P. Menzel, “The operational GOES infrared rainfall estimation technique”, *Bull. Amer. Meteor. Soc*., vol. 9, pp 1883-1898, 1998.
[6] K.L. Hsu., X. Gao, S. Sorooshian and H.V. Gupta, “Precipitation estimation from remotely sensed information using artificial neural networks”, *J. Appl. Meteor*., vol. 36, pp. 1176-1190, 1997.
[7] C. Kummerow and L. Giglio, “A method for combining passive microwave and infrared rainfall observations”, *J. Atmos. Oceanic Tecnol*., vol. 12, pp. 33-45, 1995.
[8] V. Levizzani, F. Porcù, F.S. Marzano, A. Mugnai, E.A. Smith, and F. Prodi, “Investigating a SSM/I microwave algorithm to calibrate METEOSAT infrared instantaneous rain-rate estimates” *Meteor. Applications*, vol. 3, pp. 5-17, 1996.
[9] S.W. Miller, P.A. Arkin, and R. Joyce, “A combined microwave infrared rain rate algorithm”, *Int. J. Remote Sensing*, vol. 22, pp. 3285-3307, 2001.
[10] T. Bellerby, M. Todd, D. Kniveton and C. Kidd, “Rainfall Estimation from a Combination of TRMM Precipitation Radar and GOES Multispectral Satellite Imagery through the Use of an Artificial Neural Network”, *J. App. Meteor*., vol. 39, pp. 2115-2128, 2000.
[11] F.J. Tapiador, C. Kidd, V. Levizzani, and F.S. Marzano, “A neural networks-based PMW-IR fusion technique to derive half hourly rainfall estimates at 0.1° resolution”, *J. Appl. Meteor*., vol. 43, pp. 576-594, 2004.
[12] D.I.F. Grimes, E. Coppola , M. Verdecchia, G. Visconti, “A neural network approach to real time rainfall estimation for Africa using satellite data”, *J. Hydrometeorology*, 6, 4, 1119-1133, 2003.
[13] F.S. Marzano, M. Palmacci, D. Cimini, G. Giuliani and J.F. Turk, "Multivariate statistical integration of satellite infrared and microwave radiometric measurements for rainfall retrieval at the geostationary scale", *IEEE Trans. Geosci. Remote Sens*., vol. 42, n. 4, pp. 1018-1032, 2004a.
[14] R.R. Ferraro,”SSM/I derived global rainfall estimates for climatological applications”, *J. Geophys. Res*., vol. 102, pp 16,715-16,735, 1997.
[15] S. Di Michele, A. Tassa, A. Mugnai, F.S. Marzano, P. Bauer and J.P.V. Poiares Baptista, “Bayesian Algorithm for Microwave-based Precipitation Retrieval: description and application to TMI measurements over ocean”, *IEEE Trans. Geosci. Rem. Sens.*, vol. 43, pp. 778-791, 2005.
[16] F. Dell’Acqua and P. Gamba, “Pyramidal Rain Field Decomposition Using Radial Basis Function Neural Networks for Tracking and Forecasting Purposes”, *IEEE Transactions on Geosci. and Remote Sensing*, vol. 41, no. 4, pp. 2003 853, 2003.
[17] G. Rivolta, F.S. Marzano, E. Coppola, and M. Verdecchia, “Artificial neural-network technique for precipitation nowcasting from satellite imagery”, *Adv. in Geosci*., vol. 7, pp. 97-103, 2006.
[18] Bishop C. M., *Neural Networks for Pattern recognition*, Oxford Press 1995, ISBN 0-19-853864-2
[19] T. Heinemann, A. Latanzio.,F. Roveda, The Eumetsat multi-sensor precipitation estimate (MPE), *Proceedings of the second International Precipitation Working Group (IPWG) meeting*, Madrid, Spain, September 2002.
[20] L. Cao, Practical method for determining the minimum embedding dimension of a scalar time series, Physical Review D, pp. 43-50, Dec. 1997.
[21] I. T. Jolliffe, (1986). Principal Component Analysis. *Springer-Verlag*. pp. 487. ISBN 978-0-387-95442-4..
[22] P. McCullagh, J. Nelder (1989). Generalized Linear Models, *Second Edition. Boca Raton: Chapman and Hall/CRC*. ISBN 0-412-31760-5.
[23] D. J. C. MacKay, A Practical Bayesian Framework for Backpropagation Networks, *Neural Computation,* vol.4 n°.3 pp. 448-472, 1992.
[24] F. S. Marzano, G. Rivolta, E. Coppola, B. Tomassetti, M. Verdecchia , Rainfall Nowcast from Multi-Satellite Passive Rainfall Nowcast from Multi-Satellite Passive, *TGRS-2006-00435*.
[25] Imran Maqsood et al., An ensemble of neural networks for weather forecasting, *Neural Comput & Applic* Vol. 13 pp. 112–122, 2004.
[26] www.nwcsaf.org
[27] M. Romaguera, J.A. Sobrino, G. Sria, M.M. Zaragoza, J. Cuenca, M. Gmez, J.C. Jimenez-Muñoz, A. Galdon-Ruiz, Land Surface Temperature Derived from the MSG-SEVIRI Data, *Proceedings Second MSG RAO Workshop*, Salzuburg, Austria, 9-10 Sept. 2004.
[28] Met Office, National Meteorological Library and Archive, Fact Sheet N°3, Water in the Atmosphere, August 2007.